HHS Public Access

Author manuscript

Cell. Author manuscript; available in PMC 2022 January 21.

Published in final edited form as:

Cell. 2021 January 21; 184(2): 507–520.e16. doi:10.1016/j.cell.2020.11.048.

A Circuit Logic for Sexually Shared and Dimorphic Aggressive Behaviors in *Drosophila*

Hui Chiu[1,*], **Eric D. Hoopfer**[3], **Maeve L. Coughlan**[4], **David J. Anderson**[1,2,5,*]

[1]Division of Biology and Biological Engineering 156-29, Tianqiao and Chrissy Chen Institute for Neuroscience

[2]Howard Hughes Medical Institute, California Institute of Technology, Pasadena, CA USA 91125

[3]Carleton College, 1 N. College St., Northfield, MN USA 55057

[4]Mount Holyoke College, 50 College St., South Hadley, MA USA 01075

[5]Lead Contact:

SUMMARY

Aggression involves both sexually monomorphic and dimorphic actions. How the brain implements these two types of actions is poorly understood. We have identified three cell types that regulate aggression in *Drosophila*: one type is sexually shared, and the other two are sex-specific. Shared CAP neurons mediate aggressive approach in both sexes, whereas functionally downstream dimorphic but homologous cell types, called MAP in males and fpC1 in females, control dimorphic attack. These symmetric circuits underlie the divergence of male and female aggressive behaviors, from their monomorphic appetitive/motivational to their dimorphic consummatory phases. The strength of the monomorphic→dimorphic functional connection is increased by social isolation in both sexes, suggesting that it may be a locus for isolation-dependent enhancement of aggression. Together, these findings reveal a circuit logic for the neural control of behaviors that include both sexually monomorphic and dimorphic actions, which may generalize to other organisms.

Graphical Abstract

[*]Authors for correspondence: hchiu@caltech.edu; wuwei@caltech.edu.

AUTHOR CONTRIBUTIONS

Conceptualization, D.J.A. and H.C.; Investigation, H.C. and M.L.C.; Writing - Original Draft, H.C. and D.J.A.; Writing - Review & Editing, H.C. and D.J.A.; Resources, H.C. and E.D.H.; Funding Acquisition, D.J.A.

DECLARATION OF INTERESTS

The authors declare no competing interests.

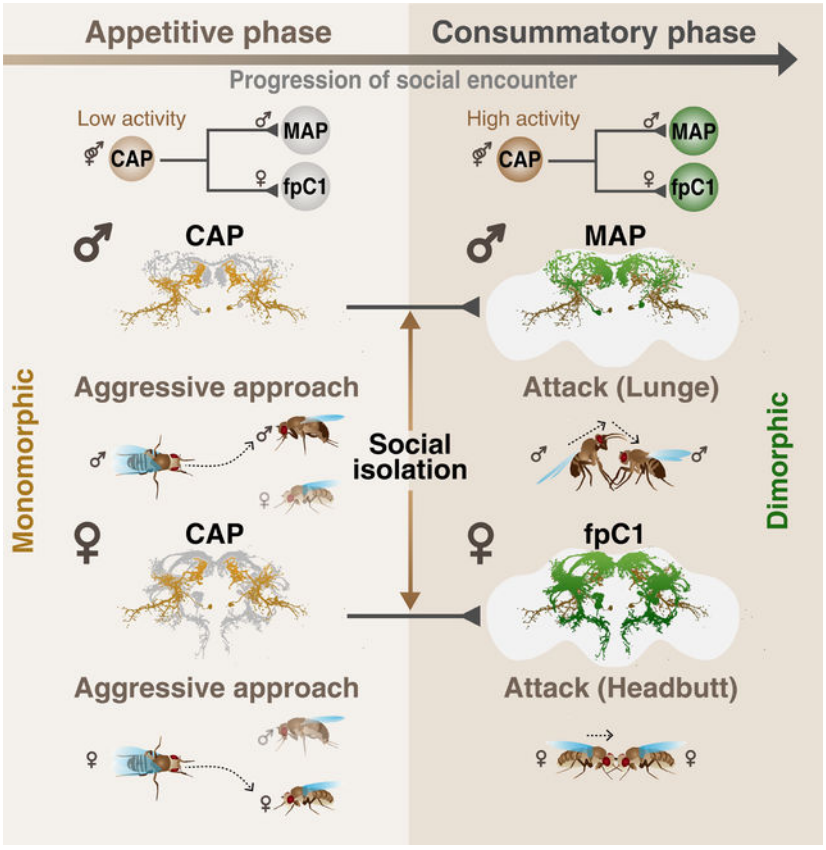

In Brief

Chiu et al. uncover how a sexually dimorphic behavior is wired in the brains of male and female flies. Looking for neuronal components controlling aggressive behaviors, they find a single type of neuron that controls aggressive approach in both sexes connected hierarchically to different neurons in males vs. females which control dimorphic attack responses (lunge vs. headbutt, respectively). They then show that social isolation, known to augment aggressive behaviors in both sexes, strengthens the connections between the monomorphic and dimorphic neurons.

INTRODUCTION

Males and females of a given species often show sex-specific differences in behavior (reviewed in Dulac and Kimchi, 2007; Manoli et al., 2013). These dimorphic behaviors can be roughly divided into two categories: “pure” dimorphic behaviors, in which males and females exhibit non-overlapping motor patterns to achieve a similar goal; and “mixed” monomorphic-dimorphic behaviors, in which certain actions are common to both sexes, while other actions are dimorphic. Extensive research in multiple species has shown that “pure” sexually dimorphic behaviors (e.g., mating) are controlled by sexually dimorphic brain circuits (reviewed in Asahina, 2018; Yamamoto and Koganezawa, 2013; Yang and Shah, 2014). However, much less is known about the configuration of circuits that control and coordinate “mixed” behaviors.

Aggressive behavior in *Drosophila* exhibits a mixed pattern: a monomorphic appetitive and a dimorphic consummatory phase (Chan and Kravitz, 2007; Chen et al., 2002; Craig, 1917; Hoyer et al., 2008; Lorenz, 1950; Nilsen et al., 2004; Vrontou et al., 2006). Both sexes approach the opponent during the appetitive phase and then initiate the consummatory attack: males lunge and tussle while females headbutt (Chan and Kravitz, 2007; Nilsen et al., 2004; Vrontou et al., 2006). A great deal has been learned about neural circuit nodes that control aggression in *Drosophila* males (reviewed in Hoopfer, 2016; Kravitz and Fernández, 2015). Less work has been done on female aggression (Deutsch et al., 2020; Palavicino-maggio et al., 2019; Schretter et al., 2020) and even less on the control of the monomorphic vs. dimorphic aspects of this behavior.

Two extreme models could explain the control of this mixed mono-/dimorphic behavior by the brain. In one model, all phases of male and female aggression are controlled by sex-specific circuit nodes. In support of this, most identified neurons controlling male and female aggression in flies are sex-specific, for example, Tk^{FruM}, aSP2 and P1a cells in males, as well as aIPg and pC1d neurons in females (Asahina et al., 2014; Deutsch et al., 2020; Hoopfer et al., 2015; Palavicino-maggio et al., 2019; Schretter et al., 2020; Watanabe et al., 2017). Furthermore, manipulation of sex-determination genes like *fruitless* or *transformer* switches the pattern of sex-specific fighting (Chan and Kravitz, 2007; Vrontou et al., 2006). In an alternative model, the mono- and dimorphic phases of aggression could be controlled by mono- and dimorphic circuit nodes, respectively. The fact that male and female aggression can be induced by common external or internal triggers (Lim et al., 2014; Ueda and Kidokoro, 2002; Wang et al., 2008) is consistent with such a model. However, sexually shared neurons that control monomorphic features of aggression have not yet been identified.

Here we identify a pair of sexually shared neurons whose activation increases aggressive approach towards same-sex targets in both males and females. We also identify homologous, male- and female-specific interneurons that promote male- or female-specific attack behavior, respectively. We show that the dimorphic neurons are functionally downstream of the common neurons in both sexes. Moreover, we demonstrate that the functional connectivity of this circuit motif is strengthened in isolated males and females, which are more aggressive than group-housed flies (Ueda and Kidokoro, 2002; Wang et al., 2008). Together, these data suggest a circuit logic for the neural control of a “mixed” monomorphic-dimorphic social behavior, and identify a potential locus for experience-dependent modulation of this behavior.

RESULTS

Fly aggression consists of sexually monomorphic and dimorphic behaviors

We first characterized aggression in wild-type flies of both sexes and developed automated classifiers for quantifying the appetitive (approach) and the consummatory (attack) phases of aggression (Figure 1; Craig, 1917; Tinbergen, 1951). An approach bout occurs similarly in both sexes, and typically involves three motor elements: orientation from a distance, advance, and contact (Figures 1A and S1A; Video S1). In contrast, attack is sexually dimorphic: in males it includes lunging, in which the behaving fly raises its upper body with

its front legs up, and slams down onto its target (Chen et al., 2002; Hoyer et al., 2008); in females it includes headbutting which comprises a quick horizontal thrust in the direction of the target fly, resulting in contact (Figure 1A; Video S2; Nilsen et al., 2004). These monomorphic (approach) and dimorphic (lunge/headbutt) aggressive behaviors could be reliably detected by our behavioral classifiers (Figure S1D; Table S2).

Aggression can be promoted by social isolation or by food in both males and females (Lim et al., 2014; Ueda and Kidokoro, 2002; Wang et al., 2008). However, direct, quantitative comparisons of these effects on the two sexes have not been performed. We therefore investigated how males and females respond to food or social isolation (SI), during or prior to aggressive encounters, respectively. Both SI and food increased aggression in both sexes, albeit to different extents (Figures 1B and 1C). However, the group-housed females showed a higher level of baseline aggression than their male counterparts (Figures 1Bi and 1Ci, GH). Thus, male and female aggressiveness can be increased by similar environmental influences, despite their dimorphic attack behavior. These influences may act in parallel on sexually dimorphic circuits (Figure 1D, Model 1), or via a module common to both sexes (Figure 1D, Model 2). To distinguish between these models, we next investigated the relationship between neural circuits controlling aggression in males versus females.

Identification of sexually shared and dimorphic aggression-promoting neurons

A distinguishing feature of Model 2 is an aggression-promoting node common to both sexes (Figure 1D, Model 2, ‘C’). We therefore searched for such neurons, by rescreening in females Gal4 drivers identified previously in a large-scale screen for aggression-promoting neurons in males (Hoopfer et al., 2015). This screen yielded a promising candidate, line R60G08-Gal4 (R60G08 neurons, henceforth), optogenetic activation of which strongly promoted both approach, and dimorphic attack, in both sexes (Figure S2A).

R60G08-Gal4 drives expression in roughly 80 neurons in males and 64 neurons in females (Figure S2B). This sex difference could reflect quantitative or qualitative differences in aggression neurons. We first confirmed that aggression is promoted by the R60G08 neurons in the brain but not in the ventral nerve cord of both sexes (Figure S2C). To narrow down the subset of neurons that controls aggression, we used an “enhancer bashing” strategy to further fractionate the R60G08 population (Figure 2A) (Hobert and Kratsios, 2019; Luo et al., 2008). To this end, we divided the 1.5-kb R60G08 *cis*-regulatory module (CRM) sequence (Jenett et al., 2012; Pfeiffer et al., 2008) into five 0.5-kb partially overlapping fragments and generated corresponding Gal4 drivers inserted into the same genomic locus (Enhancer bashing (Eb) 1–5 Gal4s).

This approach yielded new Gal4 drivers with sparse labeling of R60G08 neuron subsets in the two sexes (Figures 2B and S3A). Among these, optogenetic activation of Eb5-Gal4 neurons (Eb5 neurons, henceforth) triggered robust male and female aggression (Figures 2C), suggesting that these cells may account for R60G08 neuron-induced aggression. To test this hypothesis, we activated R60G08 neurons in the parental Gal4 driver line, while “subtracting” Eb5 neurons using Gal80 (R60G08+/Eb5−). Such activation yielded little or no detectable increase in male or female aggression (Figure S3B). These data indicate that Eb5 neurons are required for R60G08 neuron-induced aggression.

Eb5-Gal4 labeled a pair of neurons in each male hemi-brain and a single neuron in each female hemi-brain (Figure 2B). A subset of these neurons expressed *dsx-Gal4*, but none expressed FruM (Figure S3C). To further subdivide the two Eb5 neurons identified in males, we visualized their morphology using photo-activatable GFP (PA-GFP) (Datta et al., 2008; Ruta et al., 2010). This revealed two morphologically distinct cell types. One of the cell types resembled the Eb5 neuron labeled in females, whereas the other was dissimilar and appeared only in males (Figures 2Di–ii and 2Ei). We then generated intersectional drivers that separately labeled these two classes of Eb5 neurons in males, using R22F05 CRM (Figures 2Diii-v, 2Eiii, S3D, S3E, and S4Ai; Hoopfer et al., 2015). We refer to these cells as CAP (Common Aggression-Promoting neurons) and MAP neurons (Male-specific Aggression-Promoting neurons), respectively. Both the CAP and MAP drivers labeled neurons exclusively in the brain (Figure S4B).

CAP neurons promote the approach phase of aggression in both sexes

We first investigated the function of the shared CAP neurons in males and females. We optogenetically activated CAP neurons and examined the effect on interactions between pairs of freely moving group-housed (GH) flies of both sexes. When the CAP neurons were activated, both males and females initiated significantly more approach bouts during the stimulation period (Figure 3Ai). We next asked whether CAP neurons evoke generic approach towards any object, and whether approach was biased towards same- or opposite-sex flies. To this end, we developed an approach preference assay, in which we provided pairs of different “target objects” in the chamber, and asked whether the GH tester fly preferentially approached one of the targets during CAP activation. Initially, we gave each tester fly a choice between a same-sex dead fly or a fly-sized object (magnet; Figure 3Bi). Both sexes of tester flies exhibited a higher percentage of approach bouts directed toward the fly target (Figure 3Bi). This result suggests that stimulation of CAP neurons preferentially promotes approach to conspecifics, relative to an inanimate object.

We then investigated whether the approach promoted by CAP neurons was biased towards same- or opposite-sex conspecifics. *Drosophila* males normally do not attack females (even if aggression-promoting neurons are activated (Figure S5A)), and female flies of other species most frequently attack females, in competition for oviposition sites (Fernández et al., 2010; Shelly, 1999). Consistent with this, during CAP stimulation male testers preferred male over female targets, whereas female testers showed the opposite tendency (Figure 3Bii; Video S3). The tester’s target preference was not affected by the duration of its interaction with the targets prior to CAP stimulation (Figure S5B). More importantly, if both targets were female, no difference in target preference was observed between CAP-stimulated male vs. female testers (Figure 3Biii). Furthermore, wing extension, a male courtship behavior (Bennet-Clark and Ewing, 1967; von Philipsborn et al., 2011) that was induced naturally by the presence of a female (alive or dead), was not promoted by CAP activation (Figure 3Aiii). These data therefore indicate that CAP neurons promote approach towards sex-appropriate targets of aggressive behavior.

Lastly, we examined how aggression was affected in the two sexes when the CAP neurons were silenced. To do this, we enhanced natural aggressiveness using social isolation, and

silenced the CAP neurons using the inwardly-rectifying potassium channel Kir2.1 (Baines et al., 2001). Silencing the CAP neurons greatly decreased overall aggressiveness in both sexes, as indicated by a significant reduction in the number of both approach and attack bouts (Figure 3C). The locomotor activity of CAP>Kir2.1 flies was comparable to that of CAP>GFP controls (Figure S5C), suggesting that the effect to inhibit aggression is not due to a general reduction in vigor. Conditional silencing with the optogenetic inhibitor, GtACR (Mohammad et al., 2017) or the temperature-dependent inhibitory effector, Shibire^{ts}, was not feasible due to adverse effects of green light or the non-permissive temperature on aggression in control flies. Together, these data indicate that although activation of CAP neurons only promotes approach, the activity of these cells is required for both the approach and attack phases of male and female aggression. This further supports the idea that CAP neurons promote aggressive rather than generic approach.

CAP neurons exhibit sex differences in aggression-promoting thresholds

As part of our optogenetic protocol, we performed a stimulation titration experiment, in which we activated the CAP neurons in males and females with five different LED intensities titrated from 0.1 to 0.62 μW/mm^2 (Figure 4A). Unexpectedly, this experiment revealed sex differences in the threshold for CAP stimulation-induced aggression. In GH females, approach was elicited at low photostimulation intensities (0.1 μW/mm^2), while headbutting was elicited at higher intensities (0.43 μW/mm^2; Figures 4Ai ① and 4Aiii ③). By contrast, in GH males lunging behavior was not evoked, even at the highest light stimulation intensity tested (Figure 4Aiv). Furthermore, in females the threshold intensity for eliciting approach (0.1 μW/mm^2; Figure 4Ai ①) was substantially (4-fold) lower than in males (0.43 μW/mm^2; Figure 4Aii ③).

We asked what neural mechanism(s) might underlie the sex differences in the effects of CAP stimulation. We hypothesized that in females, CAP neurons might be intrinsically more excitable than in males. To test this idea, we performed an *in vivo* all-optical stimulation and imaging experiment to quantify the responses of CAP neurons to optogenetic activation in each sex (Figure 4Bi). When activated using photostimulation at the same frequency and intensity, female CAP neurons showed a slightly higher GCaMP fluorescence increase than did male CAP neurons (Figure 4Bi; p=0.034, but non-significant after the Bonferroni correction for multiple comparisons). Importantly, the fluorescence intensities of both Chrimson::tdTomato and GCaMP in the CAP neurons were statistically indistinguishable between sexes (Figure 4Bii). While this sex difference in the excitability is consistent with the observed difference in the threshold for CAP-evoked aggression, other mechanisms are likely involved.

Together, our titration experiments indicated that in GH females, CAP neurons can evoke approach and attack (headbutting), in a scalable manner. In contrast, CAP neurons only evoked approach behavior in GH males. One explanation for this difference is that in males, CAP neurons do not connect with neurons that control attack. Alternatively, they may make such a connection, but one that is weaker than in females. To distinguish these alternatives, we next sought to identify attack-promoting neurons in males and to determine their functional interaction with CAP neurons.

MAP neurons control the attack phase of aggression in males and are functionally downstream of CAP neurons

First, we asked whether MAP neurons might control the attack phase of aggression in males. Indeed, in GH males, optogenetic activation of MAP neurons strongly promoted lunging, while activation of CAP neurons was insufficient to do so (Figure 5A). Furthermore, in contrast to CAP neurons, activating MAP neurons did not increase the number of approach bouts initiated during photostimulation, relative to baseline or to genetic controls (Figures 3Aii and S4Aii). Consequently, MAP-induced lunging typically occurred during serendipitous close encounters between flies (Video S1). Consistent with these observations, the frequency of lunge bouts, but not that of approach bouts, was significantly diminished when MAP neurons were silenced using Kir2.1 (Figures 5B and S5C). To further confirm these results, we activated both CAP and MAP neurons simultaneously using Chrimson, while specifically inhibiting MAP neurons with Kir2.1 (Figure 5C). Both approach and lunging behaviors were strongly increased when CAP and MAP neurons were co-activated (Figure 2Ci–ii). The number of lunge bouts, and the fraction of approaches leading to lunges, were suppressed by MAP inhibition, but not the number of approaches initiated (Figure 5C, cf. Figure 3C). Taken together, these results suggest that the sexually shared CAP neurons are required for the initiation of approach in both males and females, while the male-specific MAP neurons are required for male-specific attack (lunging) (Figure 5E); both populations may contribute to the transition from approach to attack.

Anatomical analysis indicated that CAP and MAP neurites lie in close proximity (Figure 2Bi–ii), suggesting that MAP neurons might be a downstream target of CAP neurons in males. To test this hypothesis, we performed *in vivo* calcium imaging in MAP neurons while optogenetically stimulating CAP neurons. Indeed, GCaMP fluorescence signals in MAP neurons were significantly elevated during CAP photostimulation, suggesting that the former lie functionally downstream of the latter (Figure 6Aii). However, these experiments do not distinguish whether this functional connection is direct (monosynaptic) or indirect.

fpC1 neurons represent a functional homolog of MAP neurons in females

The foregoing results indicated that in GH males, CAP activation promotes approach, and MAP activation in turn promotes attack. Paradoxically, in GH females, strong CAP activation could evoke both approach and attack (Figures 4Aiii and 5D), but no MAP neurons were labeled by the Eb5 or MAP drivers. One explanation for this paradox is that CAP neurons in females directly control both approach and attack. Alternatively, females may contain a sex-specific homolog of MAP neurons, which was not labeled by our Gal4 drivers, and which controls headbutting (attack). We therefore searched for MAP-like neurons in females, using anatomical methods.

The morphology of the MAP cells resembles that of pC1 neurons, a cluster of cells labeled by the intersection of NP2631-Gal4 and *dsx*-Flp (Figure 2E). Thermogenetic activation of the $pC1^{NP2631;dsxFlp}$ cluster was reported to promote aggression in both males and females (Ishii et al., 2020; Koganezawa et al., 2016). NBlast (Costa et al., 2016) searches performed using MAP neurite traces as a query returned several pC1 clusters among the top hits (Figure S4C). However, MAP neurons were not labeled by NP2631-Gal4 (Figure S4D),

suggesting they might be a distinct pC1 subtype. The numbers of pC1 neurons differ in the two sexes (53–65 and 5–10 neurons per hemisphere in males and females, respectively; reviewed in Asahina, 2018), and these neurons can be further divided into morphologically distinct subtypes (Costa et al., 2016; Wang et al., 2020). This raised the possibility that a functional homolog of MAP neurons might exist among pC1 neurons in females.

Recently, a group of female-specific neurons intersectionally labeled by R26E01-Gal4 and *dsx*-Flp were shown to trigger intense female aggression when thermogenetically activated (Palavicino-maggio et al., 2019). These cells were identified as a female-specific subtype of pC1 neurons. We therefore labeled similar cells using a different intersectional strategy, in which R26E01-AD and dsx-DBD hemi-drivers were used to generate a split-Gal4 (Figure 6Bi). Cells labeled by this split-Gal4 driver in females exhibited a main projection pattern similar to that of MAP neurons, but additionally extended a short, lateral branch and a long, ventral branch (cf. Figure 6Ai vs. 6Bi). No neurons were labeled in the male brain (Figure S4Ei). The overall morphology of these cells resembles that of pC1d neurons, a subtype of pC1 neurons that recently has been shown to promote female aggression (Deutsch et al., 2020; Schretter et al., 2020; Wang et al., 2020). We therefore refer to these neurons as “fpC1” cells. Unfortunately, it was not possible to establish definitively correspondence between fpC1 and pC1d neurons, due to driver incompatibility. Because of their anatomic similarity to MAP neurons in males, these data raised the possibility that fpC1 neurons might be female analogs or homologs of MAP neurons.

Because previous studies of R26E01-Gal4; dsx-FLP neurons used thermogenetic activation, and did not include analysis of approach behavior (Palavicino-maggio et al., 2019), we first activated these neurons optogenetically (Figure 6C). Such activation promoted female attack (headbutting; Figure 6Cii), but not approach behavior (Figure 6Ci). We confirmed that this phenotype is due to activation of fpC1 neurons in the brain, but not of those in the ventral nerve cord (Figure S4Eii). Finally, we silenced fpC1 neurons using Kir2.1. This manipulation strongly suppressed headbutting, but did not affect approach (Figures 6D and S5C). Thus, the behavioral phenotype of activating and silencing fpC1 neurons in females was analogous to that of activating and silencing MAP neurons in males (Figures 3Aii, 5Aii, and 5B).

Since MAP neurons receive excitatory input from CAP neurons in males, we hypothesized that fpC1 neurons may likewise receive excitatory input from CAP neurons in females. Indeed, fpC1 neurons responded strongly to CAP activation (Figure 6Bii), suggesting that they are indeed direct or indirect synaptic targets of the latter cells. Next, we performed a behavioral epistasis experiment, in which CAP neurons were strongly activated while silencing fpC1 neurons with Kir2.1 (Figure 6E). In this compound genotype, CAP-induced female aggression was suppressed. Together, these data suggest that fpC1 neurons are functionally as well as physiologically downstream of CAP cells in females. If so, it would suggest an analogous circuit motif controlling aggression in the two sexes, in which the sexually shared CAP neurons target MAP neurons in males, and fpC1 neurons in females (Figure 6F).

We observed that CAP stimulation caused a relatively greater increase in ΔF/F in fpC1 than in MAP neurons (Figures 6Aii vs. 6Bii, Stim). This difference was not due to sex differences in Chrimson expression in CAP neurons (Figure 4Bii), or in baseline GCaMP expression in MAP vs. fpC1 neurons (Figure S4F). One possibility is that the CAP→fpC1 functional connection in females is stronger than the CAP→MAP connection in males. This would be consistent with our observation that strong CAP activation in GH females evoked both approach and attack, while in GH males it evoked only approach. Alternatively, fpC1 neurons may be intrinsically more excitable than MAP neurons.

Social isolation enhances aggressiveness by strengthening circuit connectivity

The effect of social isolation to increase aggression has been observed in many species (Chiara et al., 2019; Toth et al., 2008; Ueda and Kidokoro, 2002; Wang et al., 2008; Zelikowsky et al., 2018). We thus wondered how social isolation can boost aggressiveness in both males and females, despite their differences in aggression circuitry and behavior. Social isolation may act to increase the excitability of CAP neuron in both sexes, the excitability of both MAP and fpC1 neurons, or the strength of the connection between CAP→MAP/fpC1 neurons. To address this, we investigated the excitability and functional connectivity of these neurons in group- (GH) vs single-housed (SH) flies.

We first compared the excitability of each of the three neuron types in GH vs. SH flies, by co-expressing Chrimson and GCaMP in each cell, and optogenetically activating and imaging them. In both sexes, the response amplitude of each of these neurons to direct activation was comparable in SH versus GH flies (Figure S6). We next imaged MAP or fpC1 neurons while optogenetically stimulating CAP neurons. In both sexes, the response of MAP/fpC1 neurons to CAP activation was significantly greater in SH than in GH flies (Figure 7A). These results suggest that the CAP→MAP functional connection in males, and the CAP→fpC1 functional connection in females, may be strengthened by social isolation.

To examine the behavioral consequences of this enhanced functional connectivity, we optogenetically activated CAP neurons in SH flies of both sexes (Figures 7B and 7C), at the lowest photostimulation intensity used for GH flies in our titration experiment (Figure 4A). SH flies exhibited increased approach behavior in both sexes, in comparison to GH flies (Figures 7Bi and 7Ci, GH→SH, ‘ChR’). More importantly, in both sexes, weak activation of CAP neurons in SH flies triggered both approach and sex-specific attack behaviors (Figures 7Bii and 7Cii, GH→SH, ‘ChR’), a phenotype not observed in GH flies of either sex at this stimulation intensity (Figures 7Bii and 7Cii, GH→GH, ‘ChR’). Thus, in SH males, weak activation of CAP neurons promoted both approach and lunging, a response not observed in GH males even at the highest photostimulation intensity tested (Figure 4Aiv). Taken together, our *in vivo* imaging analyses and behavioral experiments support the conclusion that social isolation elevates aggressiveness in both sexes, at least in part, by strengthening the functional connectivity between CAP neurons and their downstream MAP/fpC1 targets.

DISCUSSION

How behaviors that exhibit sexually monomorphic, as well as dimorphic, action components are implemented in the brain is poorly understood. Here we have identified three cell types

that regulate aggression in *Drosophila*: one type is sexually shared, and the other two are sex-specific. The shared cell type, called CAP neurons, mediates aggressive approach in both sexes, and in turn activates the dimorphic cell types, called MAP in males and fpC1 in females, which control dimorphic attack (Figure 7D). These mirrored circuit motifs therefore underlie the divergence of male and female aggressive behaviors, from their monomorphic appetitive/motivational to their dimorphic consummatory phases. This circuit logic may generalize to other behaviors and organisms.

Dissociable neural control of aggressive approach vs attack

The results presented here suggest that in both sexes, the approach vs. attack phases of aggression are controlled by different neuron types. Importantly, the approach behavior controlled by CAP neurons is directed preferentially towards same-sex conspecifics, and is required for natural attack, arguing that it expresses aggressive motivation, and not simply generic social investigation. However, this conclusion presents a seeming paradox: if approach behavior is required for attack during natural aggression, how can experimental MAP stimulation cause attack without promoting approach behavior as well?

Close examination of fighting patterns during MAP stimulation suggests an explanation for this paradox. Tester males lunged during MAP stimulation only when the target fly was in close proximity. Such proximity resulted from both directed approaches, and through serendipitous close encounters, such as when a climbing target fly fell off the chamber wall next to the tester (Video S1). The relatively small arenas (16mm in diameter) used in our experiments increased the frequency of the latter type of events. Indeed, the majority (75%) of lunge bouts promoted by MAP stimulation occurred following such serendipitous close encounters. Moreover, once an initial MAP-evoked lunge occurred, tester males could perform lunges continuously towards the target as long as it remained in proximity (Figure S5D). In this way, MAP stimulation can promote lunging without also promoting approach.

We find that approach and attack are triggered at progressively higher stimulation intensities. Other studies have shown that a single pair of descending neurons controls sequential male courtship actions in a ramp-to-threshold manner (McKellar et al., 2019). Our observations are consistent with such a mechanism operating to control the transition from approach to attack, but further studies will be required to validate this hypothesis (Figure 7E). Similarly, in mammals, optogenetic stimulation of estrogen receptor 1-positive ($Esr1^{+}$) neurons in the ventrolateral subdivision of the ventromedial hypothalamus (VMHvl) has been shown to promote sniffing/mounting and attack at low vs. high thresholds, respectively (Lee et al., 2014). However calcium imaging has revealed substantial overlap between attack- vs. sniff-tuned $VMHvl^{Esr1+}$ neurons (Remedios et al., 2017). In contrast, distinct populations of neurons in the lateral hypothalamus (LH) have been shown to be active during the appetitive vs. consummatory phases of feeding behavior (Jennings et al., 2015). Whether these distinct populations are functionally interconnected, and whether they control their respective behaviors at different thresholds, is not yet clear.

Physiological sexual dimorphisms in anatomically similar circuits

Despite the overall similarity in circuit logic between males and females, the light-intensity threshold for optogenetically induced CAP-mediated approach is lower in females. Our data indicate that this difference may reflect, at least in part, a higher intrinsic excitability of CAP cells in GH females than in males. This difference may also explain why wild-type GH females are more aggressive than wild-type GH males (Figures 1Bi and 1Ci, GH), although further studies are required to confirm this.

In addition, the intensity threshold for attack stimulated by optogenetic activation of CAP cells is lower in females than in males, particularly in GH flies where stimulation of CAP neurons in males does not promote attack at all (Figure 4A). In SH flies, however, attack as well as approach could be evoked by CAP stimulation in both sexes (Figures 7B and 7C). One explanation for this sex difference is that in GH males, the threshold for MAP activation by CAP cells is higher than the threshold for fpC1 activation in females. In SH males, however, because the excitability of the CAP→MAP connection is enhanced, this threshold can be reached and therefore lunging can be evoked by CAP stimulation (Figures 7Ai and 7Bii). The synaptic basis for this physiological dimorphism remains to be investigated.

Dimorphic but homologous pC1 neuron subtypes may control dimorphic aspects of aggressive behavior

The symmetry between the CAP→MAP circuit in males and the CAP→fpC1 circuit in females raises the question of whether MAP and fpC1 neurons are sex-specific, analogous cell types. pC1 neurons, a large (~50-cell) cluster of *doublesex*-expressing cells labeled by NP2631-Gal4 (Koganezawa et al., 2016), promote both male and female aggression (Ishii et al., 2020; Koganezawa et al., 2016). More recent studies have suggested that a sex-specific subpopulation of pC1 neurons, called pC1d, controls aggression in females (Deutsch et al., 2020; Palavicino-Maggio et al., 2019; Schretter et al., 2020; Wang et al., 2020). These cells resemble fpC1 cells (Figure 6Bi); although establishing correspondence between these pC1 subtypes is currently challenging, due to Gal4 driver incompatibility and the multiplicity of morphologically similar cell types within a cluster.

Our data suggest that MAP neurons may represent a male-specific subclass of pC1 neurons. Although MAP neurons are not labeled by NP2631-Gal4 (Figure S4D), the cell body location and the morphology of these cells appear similar to that of some pC1 neurons (Figure 2Eiv), an observation supported by NBlast analysis (Figure S4C). MAP and fpC1 neurons share their main projection patterns, but the latter have two extra branches projecting laterally and ventrally (Figures 6Ai and 6Bi). This suggests that these two cell types are indeed functional homologues. This point should be further clarified once an EM-level connectome of the male fly brain is available.

Relationship to other aggression-promoting neurons

While our data provide an overall logic for the functional organization of male vs. female aggression circuits, they leave out the details of its implementation. For example, it is not yet clear whether CAP→MAP/fpC1 connections are direct or indirect, and exclusively feed-forward or also recurrent. Our initial examination of the female EM connectome identified

several candidate CAP-like neurons, some of which make direct monosynaptic connections with fpC1-like pC1d neurons. pC1d neurons in turn connect to aIPg neurons, which also promote female aggression; however there is extensive recurrence between pC1d and aIPg cells (Deutsch et al., 2020, Schretter et al., 2020).

Although a male EM connectome is not yet available, several other groups of male-specific neurons, such as the $FruM^{+}$ Tachykinin(Tk)-expressing neurons, have been previously shown to play important roles in male aggression (Asahina et al., 2014; Hoopfer, 2016; Kravitz and Fernández, 2015). Whether and how these male-specific neurons interact with CAP and MAP neurons to regulate male aggression remains largely unexplored. Initial epistasis experiments suggest that Tk neurons act downstream of the Eb5 (CAP+MAP) neurons to regulate aggression (Figure S7). In the future, it will be interesting to clarify the implementation of connectivity between CAP, MAP, and Tk neurons once a male connectome becomes available. Nevertheless, the functional pathways defined by CAP and MAP/fpC1 neurons establish a conceptual framework for understanding how monomorphic and dimorphic aggressive behaviors are regulated in the two sexes.

Dimorphic aggressive behavior and internal states

A fundamental question that emerges from the sexual dimorphism in fly aggressive behavior (Nilsen et al., 2004; Vrontou et al., 2006) is whether the central motive state of aggressiveness is encoded similarly or differently in the two sexes. Our data suggest that CAP neurons might be candidates for controlling an internal state of aggressiveness that is common to both sexes. Two lines of evidence support this idea. Firstly, CAP stimulation promotes the appetitive phase of aggression (Figure 3B). In other systems, the appetitive phase of goal-directed behaviors has been shown to reflect an internal state of motivation or drive (Gentry et al., 2019; Jennings et al., 2015; Salamone and Correa, 2012). Secondly, in SH flies CAP neurons are able to evoke not only approach, but also attack, in both sexes. The ability of CAP neurons to control different phases of aggression, in a scalable manner (Figure 7E), is reminiscent of the function of $VMHvl^{Esr1+}$ neurons in mice (Falkner et al., 2014; Falkner et al., 2016; Lee et al., 2014; Remedios et al., 2017; Yang et al., 2013); these cells have been suggested to mediate an aggressive internal state (Anderson, 2016; Anderson and Adolphs, 2015; Hashikawa et al., 2016).

Finally, our findings raise the question of whether sexually dimorphic attack neurons, analogous to MAN and fpC1, are present in other species. In rodents, males and females attack different body parts of a same-sex intruder (Blanchard et al., 1975; Sgoifo et al., 1992). This topographic difference in biting may reflect sexual dimorphisms in other aspects of rodent aggression that have not yet been fully characterized. Whether this behavioral dimorphism reflects underlying sex differences in the neural control of attack is also unclear. In mice, Esr1/progesterone receptor-expressing ($Esr1^{+}/PR^{+}$ neurons) glutamatergic neurons in VMHvl have been shown to control both male and maternal aggression (Hashikawa et al., 2017; Lee et al., 2014; Yang et al., 2013). However, recent single-cell RNA sequencing data have revealed at least 7 distinct transcriptomic cell types among $VMHvl^{Esr1+/PR+}$ neurons, some of which are male- or female-specific (Kim et al., 2019). Several of these cells types are specifically activated during aggression, including one that is male-specific. Which

transcriptomic cell type(s) is activated during maternal aggression is not yet clear. Thus, whether the same or different cell types regulate male vs. female aggression in vertebrates, as well as how different phases of aggressive behavior are regulated in each sex, remains to be determined.

STAR METHODS

RESOURCE AVAILABILITY

Lead Contact—Requests for resources and reagents should be addressed directly to the Lead Contact, David J. Anderson (wuwei@caltech.edu).

Materials Availability—The plasmids and the transgenic flies generated in this study are available upon request. They will also be deposited to Addgene and the Bloomington stock center, respectively. The behavioral classifiers are available to download: https://github.com/H-Chiu/Classifiers.

Data and Code Availability—Source data and analysis codes supporting this study are available upon request.

EXPERIMENTAL MODEL AND SUBJECT DETAILS

Fly strains—Canton-S (from the lab of Dr. Martin Heisenberg) was used as the wild type. Please see Table S1 for the full genotypes of flies used in each figure and see the Key Resource Table for the source of these flies. Briefly, R60G08-Gal4(attp2), pBDPGal4U(attp2), BDP-p65AD(attp40), BDP-Gal4DBD(attp2), R22F05-Gal4DBD(attp2), 20xUAS-IVSSyn21-GFP(attp2), 10xUAS-eGFP::Kir2.1(attp2), 10xUAS-IVS-Syn21-GFP(attp2), 20xUAS-FRT-myrTopHat2-FRT-Chrimson::tdT3.1(vk5), 20xUAS-IVS-Syn21-Chrimson::tdT3.1 (su(Hw)attp5 and vk5), 13xLexAop2-CsChrimson::tdT3.1(vk5), 13xLexAop2-Chrimson::tdT3.1(su(Hw)attp5), 13xLexAop2-eGFP::Kir2.1(attp40), 10xUAS-nls::tdTomato(vk22), 10xUAS-nls::GFP(vk40) were kindly shared by the Gerald Rubin laboratory (HHMI Janelia Research Campus) and Barret Pfeiffer. *dsx*-Gal4, *dsx*-Flp, *dsx*-DBD were kindly shared by the Stephen Goodwin laboratory (University of Oxford, UK). NP2631; dsx-Flp was kindly shared by the Daisuke Yamamoto laboratory (Tohoku University, JP). R26E01-Gal4(attp2)(RRID:BDSC_60510), R26E01-p65AD(attp40) (RRID:BDSC_75740), 20xUAS-IVS-CsChrimson-mVenus(attp2) (RRID:BDSC_55136), 20xUAS-IVS-jGCaMP7b(vk5) (RRID:BDSC_80907), 13xLexAop-IVS-jGCaMP7b(vk5) (RRID: BDSC_80915) were obtained from the Bloomington Stock Center (Indiana University).

Rearing conditions—Stocks and crosses were reared at 25°C and 50% humidity and maintained on a 12hr:12hr light:dark cycle. To keep the fly density consistent across experiments, each cross was set up with 10–12 virgin females and 5–6 males, and was flipped every two days. Experimental flies were collected mostly as virgins on the same day of eclosion and reared in isolation (single-housed (SH) condition; one fly per vial), or in groups (group-housed (GH) condition; ~20 single-sex flies per vial). For optogenetic experiments, flies were transferred to vials containing retinal food (regular fly food mixed

with all-trans-retinal to a final concentration of 0.2 mM) after collection and reared in the dark for 5–6 days. Flies were flipped to fresh retinal food vials one day before a behavioral test.

Construction of transgenic animals—Several strains were generated for this study: Eb2-Eb5-Gal4s, Eb5-p65AD, Eb5-Gal80, R22F05-Gal80, R22F05-LexADBD, and Eb5-iLexA (improved LexA). Enhancer-bashing fragments, Eb2-Eb5, were PCR-amplified from R60G08 sequence (Jenett et al., 2012; Pfeiffer et al., 2008) and cloned into pBPGUw (Addgene #17575) via Gateway and the LR reaction. A detailed description of the cloning strategy can be found in Pfeiffer et al., 2008. Sequences of the primers used for PCR amplification are listed in the key resources table. The Eb5 fragment was subcloned into pBPp65ADZpUw (Addgene #26234) and pBPGAL80Uw-6 (Addgene# 26236) to generate Eb5-p65AD and Eb5-Gal80, respectively. To make the construct R22F05-Gal80, the R22F05 fragment was first amplified from the genomic DNA of the reference strain (Adams et al., 2000) using the primers listed in the 'Janelia_info' excel sheet (Jenett et al., 2012; downloaded from Bloomington Stock Center webpage: https://bdsc.indiana.edu/stocks/gal4/gal4_janelia.html) and then cloned into pBPGAL80Uw-6 via Gateway and the LR reaction. To improve the strength of LexA, we fused the activating domain of Gal4, GAD, to the C-terminus of nlsLexA::p65 (Addgene #26230) to make pBPnlsLexA::p65::GADUw. The GAD sequence was amplified from the pBPGUw. It has been shown that the expression of a targeted gene can be enhanced by adding additional activating domains to its transcription activator (Chavez et al., 2016). The Eb5 fragment was then cloned into pBPnlsLexA::p65::GADUw via Gateway and LR reaction to create Eb5-iLexA. All constructs were verified by sequencing. To make the construct R22F05-LexADBD, we first generated the pBPZpnlsLexADBD construct. A nlsLexADBD fragment was PCR-amplified from pattB-nsyb-MKII::nlsLexADBDo (Addgene #64725) and cloned into pBPZpGal4DBD (Addgene #26233) plasmid using KpnI and HindIII sites. The R22F05 enhancer fragment was then cloned into pBPZpnlsLexADBD via Gateway and LR reaction.

METHODS DETAILS

Immunohistochemistry and brain registration—Brains or ventral nerve cords of 6–8 day old flies were dissected in cold PBS and fixed in 4% paraformaldehyde for 1 hour at 4°C. After fixation, samples were washed twice with 0.05% PBST (PBS containing 0.05% Triton X-100) for 15 minutes at room temperature (RT), and incubated in 2% PBST (PBS containing 2% Triton X-100) at RT for 30 minutes. Samples were then blocked in 5% normal goat serum (NGS) solution for 2 hours or overnight at 4°C. After blocking, samples were incubated with the primary antibody solution for two days at 4°C. The dilution ratios for the primary antibodies used in this study were 1:1000 for anti-GFP or anti-RFP and 1:20 for nc82 or anti-NCad. To obtain even labeling of the neuropils, which is critical for subsequent brain registration, samples were transferred to freshly diluted primary antibody solution on the second day of incubation. Afterwards, the samples were washed with 0.05% PBST for 30 minutes at 4°C three times and then incubated with the secondary antibody solution for two days at 4°C. All secondary anti-bodies used in this study were diluted 1:1000. Finally, the samples were washed three times with 0.05% PBST for 30 minutes at 4°C and incubated overnight in the mounting media Vectashield (Vectorlabs, Inc.) at 4°C.

Image stacks were obtained using confocal microscopy (Olympus Fluoview FV1000 or FV3000). Representative images illustrating the expression patterns of each driver were chosen from among 6–10 dissected samples. Brain images were first registered to JFRCtemplate2010 (Jenett et al., 2012) using the CMTK registration GUI (Jefferies et al., 2007; Masse et al., 2012) and z-projected with maximum intensity under Fiji. To create overlays of two registered brain images, images were pseudocolored and layered in Photoshop.

Behavioral assays—Details for each of the five different assays performed in this paper are listed below. In general, all experiments were performed in a room maintained at 25°C and 50% humidity. The behavioral chamber is a 12mm-high 16mm-diameter acrylic cylinder with a clear top and floor. The wall and the lid of the chambers were coated with Insect-A-Slip and silicon fluid, respectively. The floor was covered with freshly prepared apple juice agar (2.5% (w/v) sucrose and 2.25% (w/v) agarose in apple juice) and illuminated with an 850nm backlight (SOBL-200×150–850, SmartVision Lights, Muskegon, MI). Flies were tested on the 6^{th} or 7^{th} day after eclosion. Flies were introduced into the chambers by gentle mouth pipetting and allowed to settle for at least two minutes before the tests began. Behaviors were recorded at 30fps from the top using a Point Grey Flea3 camera with a long pass IR filter (780 nm, Midwest Optical Systems).

Group-housed (GH) vs. single-housed (SH) assay.: Canton-S males and females were collected on the day of eclosion and reared in the single-housed (one per vial; SH) or group-housed (twenty single-sex flies per vial; GH) condition. In each behavior chamber, we paired same-sex flies from different vials to avoid the influence of prior life history, e.g. a GH male from the first vial 1 was paired with a GH male from the second vial. Interactions were recorded for 10 minutes.

Food vs. no food assay.: Canton-S males and females were collected on the day of eclosion and reared in group-housed condition until the test day (the 6^{th} day after eclosion). Same-sex flies were paired in the chambers with or without a freshly prepared banana chunk (~$2mm^3$) in the center as the food resource, where indicated.

Optogenetic stimulation assay.: Experimental flies were group-housed and raised on retinal food in the dark until the test day. Flies were transferred to fresh vials one day before the experiment. A detailed description of the photostimulation setup can be found in Inagaki et al., 2014. Briefly, a high-powered 655nm LED was mounted ~8cm above the chamber at a 24° angle to provide photostimulation at various intensities and frequencies. With the exception of the stimulation titration experiments shown in Figure 4, 10 Hz and 5Hz pulsed light with a maximum intensity = 0.62 $\mu W/mm^2$ were used to activate neurons in males and females, respectively. The stimulation protocol included a 30s baseline activity recording, two 30s stimulation blocks separated by a 30s interstimulation interval, and a 30s post-stimulation period. Behaviors observed during experiments were present as the average from two stimulation blocks. For the stimulation titration experiment shown in Figure 4A, the same set of experimental flies were tested with 5 different intensities of photostimulation (0.1–0.62 $\mu W/mm^2$) using the same stimulation paradigm. The order of the intensity was

randomly applied and each experiment was followed by a 5min interval to allow the experimental flies to recover to their baseline activity. Data were collected from two independent sets of experimental flies.

Preference assay (Figure 3B).: The chamber used was a 12mm-high cylinder with a 16mm diameter. The two targets were mounted at the opposite sides of the floor, ~10mm apart using a UV glue tool kit (Bondic). For Figure 3Bi, the left and the right targets were a fly (same-sex as the tester) and a fly-size magnet (K&J Magnetics, Pipersville, PA; Cylinder 1/16"x1/16", D11-N52), respectively. The fly targets were 5–6-day old Canton-S virgin males or females frozen at −80°C for 20 minutes immediately before the experiment. For Figure 3Bii, the male and the female fly targets were mounted at the left and the right sides of the chamber, respectively. For Figure 3Biii, the left and right targets were both females. Testers were introduced into the chamber from the top and were allowed to freely explore the arena and the targets for two minutes before the standard optogenetic stimulation (30s pre-stimulation period followed by 30s 655nm photostimulation) was applied. The preference index was calculated as follows,

$$\text{preference index} = \frac{n_{\text{left}} - n_{\text{right}}}{n_{\text{left}} + n_{\text{right}}},$$

where n_{left} is the number of approach bouts toward the left target and n_{right} is the number of approach bouts toward the right target.

Loss-of-function assay.: The inwardly-rectifying potassium channel Kir2.1 was expressed in CAP (Figure 3C), MAP (Figures 5B–C), fpC1 (Figures 6D–E), Tk (Figure S7A), and Eb5 (Figure S7B) neurons to test how silencing these neurons affects naturally- or artificially-induced aggression. Experimental flies were single-housed for six days under a normal 12hr-light: 12hr-dark cycle to naturally enhance aggressiveness (Figures 3C, 5B, and 6D). For behavioral epistasis experiments where fighting was optogenetically induced experimental flies were group-housed and reared in dark (Figures 5C, 6E, and S7).

Optogenetic activation in isolated flies experiment (Figures 7B–C).: GH>GH flies and GH>SH testers were collected on the same day. Both fly groups were reared in the GH condition for the first three days. On the fourth day, the control (GH>GH) flies were transferred to a new vial and maintained in groups whereas the testers (GH>SH) were isolated individually; both groups were maintained for an additional 3 days. The optogenetic stimulation experiments were done on the morning of the 7$^{\text{th}}$ day. Here we purposely shortened the length of social isolation from six days (our standard procedure; Wang et al., 2008) to three days, in order to avoid a ceiling effect on aggression.

Functional imaging—Six-day old experimental flies were briefly anesthetized on ice and head-fixed on a customized holder with the UV glue in their normal standing posture. The top of the fly head was immersed in fly saline (103mM NaCl, 3mM KCl, 5mM N-Tris(hydroxymethyl)methyl-2-aminoethane-sulfonic acid, 8mM trehalose, 10mM glucose, 26mM $NaHCO_3$, 1mM NaH2PO_4, 4mM MgCl2, 1.5mM CaCl2; pH7.25; 270–275mOsm)

(Hong and Wilson, 2015). A piece of cuticle (~350 μm by 350 μm) was removed from the posterior side of the head capsule to create an imaging window. After surgery, the experimental fly was placed under a 0.8 numerical aperture (NA) 40x objective (LUMPLFLN40XW, Olympus) and habituated for at least 5 minutes. The optical setup for two-photon imaging with optogenetic activation was as described in Inagaki et al., 2014. Briefly, imaging was performed using a custom-modified Ultima two-photon laser scanning microscope (Bruker). 920nm ultrafast light pulses for exciting GCaMP was provided by a Chameleon Ultra II Ti:Sapphire laser (Coherent) and the GCaMP signals were detected by photomultiplier-tubes (Hamamatsu). Images were acquired at 256×256 pixel resolution and 2 frames per second. Chrimson activation was provided by a fiber-coupled 660nm LED (M660F1, Thorlabs), powered by a 1-channel LED driver with pulse modulation (DC2100, Thorlabs) and delivered through an optical fiber (200μm in diameter, 0.39NA, M75L01, Thorlabs) placed above the imaging window at a ~45° angle and ~500μm in distance. The stimulation paradigm included a 20s baseline, 5s photo-stimulation at the designated frequency (5–50Hz) and intensity (0–34.6 μW), and a 35s post-stimulation period.

Labeling neurons with photoactivatable GFP—To trace the morphologies of different Eb5 cell classes, photoactivatable-GFP (PA-GFP; Datta et al., 2008; Ruta et al., 2010) was expressed by Eb5-Gal4 (attp2) in both sexes. The experimental preparation was similar to functional imaging experiments except that the photoactivation was provided by 710 nm ultrafast light pulses using the two-photon microscope. The photoactivation was first localized to the cell body of the targeted neuron and, after the diffusion of the activated PA-GFP, applied subsequently to the terminus of the labeled segments to extend the labeling. Photoactivation cycles were separated by 10min intervals to allow the spread of activated PA-GFP and the entire experiment typically lasted 1.5–2 hours for each cell. Image stacks were taken at 1024×1024 pixel resolution. For the purpose of clarity, the labeled neuron was traced with Simple Neurite Tracer plugins using Fiji to mask the background fluorescence. The morphology of each cell class was confirmed with at least two biological replicates.

QUANTIFICATION AND STATISTICAL ANALYSIS

Statistics and quantification—Statistical analysis was performed using MATLAB. All behavioral data were compared using nonparametric tests. The n number for each experiment is indicated in the figures and listed in Table S3, along with the statistical method used for each comparison, the *p*-value, and the test scores. Briefly, Mann-Whitney U-tests and Wilcoxon signed-rank tests were used for between and within-group comparisons, respectively. The cutoff for significance was set as an $\alpha<0.05$. The central mark of each boxplot indicates the median and the bottom and top are the 25^{th} and the 75^{th} percentiles, respectively.

Fly tracking and behavior classification—Behavioral videos were tracked with Caltech FlyTracker to determine the positions, the velocities, and the postures of the experimental flies in 30 fps recordings (Eyjolfsdottir et al., 2014). These tracking data were used by behavioral classifiers developed with the Janelia Automatic Animal Behavior Annotator (JAABA; Kabra et al., 2013) to determine the behavioral bouts. Naturally occurring fighting between single-housed male-male or female-female wild-type pairs were

used to train the classifiers. We used the following criteria to train the classifiers for approach, lunge, and headbutt, separately: An approach bout starts when the two flies are at a distance (at least one fly-body length(~3mm) apart). The behaving fly first orients toward the target fly, moves forward with acceleration, and finally makes contact with the target (e.g., their legs are crossing or their bodies touching). We used the same approach classifier for detecting male and female approach bouts, and classifier performance was comparable between the two sexes (Figure S1D). We considered lunging and headbutting as short-distance behaviors. The behaving fly only lunges or headbutts when the target fly is in close proximity. Also, lunging and headbutting are very brief actions whereas the duration of approach may vary depending on the distance and the velocity of the behaving fly. A lunge bout begins when the behaving fly raises its front legs and its upper body and "slams down" onto the target fly. We consider lunging as a male-specific behavior because it was only observed during male fights in our experiments; application of the automated lunge classifier to videos of female fights yielded only false positives. A headbutt bout was scored when the behaving fly lashed out in a thrust with its head, towards the target. The classifier performance is listed in Table S2. Behavioral bouts annotated by the classifiers were manually curated to eliminate false-positives and false-negatives in all experiments.

Imaging data analysis—Same-size region of interests (ROIs) were manually drawn over the cell bodies of targeted neurons and the GCaMP fluorescence in the ROIs was measured using the ROI manager in Fiji software. The mean of the fluorescence intensity during the first 20s of image acquisition was used as the baseline fluorescence (F) to calculate the ΔF/F. The ΔF/F was then normalized to the maximum peak value of fluorescence detected within the full data set that combined data from all genotypes involved, and is presented as ΔF/F (%). The mean of ΔF/F during the indicated periods (5s before, during, and after photo-stimulation) was calculated and compared using the Wilcoxon signed-rank (WSR) test and Mann-Whitney U (MWU) test in MATLAB. Specifically, MWU was used for between-genotype comparison whereas WSR was used for within-genotype pre-stimulation (Pre-stim) versus during stimulation (Stim) comparisons. The cutoff for significance was set as $\alpha<0.05$. Each data point represents one cell per fly. For each genotype, the testing flies were collected from two independent crosses to avoid sampling bias.

Supplementary Material

Refer to Web version on PubMed Central for supplementary material.

ACKNOWLEDGMENTS

We thank Dr. J.-Y. Yu for editing the draft and discussions; Drs. Y. Jung and J.-Y. Yu for advice on imaging experiments; Drs. G.M. Rubin and B. Pfeiffer for unpublished reagents; Dr. B.J. Dickson for FruM antibody. Dr. S.F. Goodwin for *dsx* drivers. Drs. H.T. Schwartz, E.J. Hong, C. Lois, P. Sternberg, members of the Anderson laboratory for valuable comments on the manuscript; A. Sanchez for fly maintenance; C. Chiu, G. Mancuso, and X. Da for laboratory management and administrative assistance. This work was supported by NIDA Grant R01-DA031389 and D.J.A. is an Investigator of the Howard Hughes Medical Institute.

REFERENCES

Adams MD, Celniker SE, Holt RA, Evans CA, Gocayne JD, Amanatides PG, Scherer SE, Li PW, Hoskins RA, Galle RF, et al. (2000). The genome sequence of *Drosophila melanogaster*. Science 287, 2185–2195. [PubMed: 10731132]

Anderson DJ (2016). Circuit modules linking internal states and social behaviour in flies and mice. Nat. Rev. Neurosci 17, 692–704. [PubMed: 27752072]

Anderson DJ, and Adolphs R (2015). A framework for studying emotions across phylogeny. Cell 157, 187–200.

Asahina K, Watanabe K, Duistermars BJ, Hoopfer E, Gonzalez CR, Eyjolfsdottir EA, Perona P, and Anderson DJ (2014). Tachykinin-expressing neurons control male-specific aggressive arousal in *Drosophila*. Cell 156, 221–235. [PubMed: 24439378]

Asahina K (2018). Sex differences in *Drosophila* behavior: qualitative and quantitative dimorphism. Curr. Opin. Physiol 6, 35–45. [PubMed: 30386833]

Baines RA, Uhler JP, Thompson A, Sweeney ST, and Bate M (2001). Altered electrical properties in *Drosophila* neurons developing without synaptic transmission. J. Neurosci 21, 1523–1531. [PubMed: 11222642]

Bennet-Clark HC, and Ewing AW (1967). Stimuli provided by courtship of male *Drosophila* melanogaster. Nature 215, 669–671.

Blanchard RJ, Fukunaga K, Blanchard DC, and Kelley MJ (1975). Conspecific aggression in the laboratory rat. Comp. Physiol. Psychol 89, 1204–1209.

Cachero S, Ostrovsky AD, Yu JY, Dickson BJ, and Jefferis GS (2010). Sexual dimorphism in the fly brain. Curr. Biol 20, 1589–1601. [PubMed: 20832311]

Chan Y-B, and Kravitz EA (2007). Specific subgroups of FruM neurons control sexually dimorphic patterns of aggression in *Drosophila melanogaster*. Proc. Natl. Acad. Sci. USA 104, 19577–19582. [PubMed: 18042702]

Chavez A, Tuttle M, Pruitt BW, Ewen-Campen B, Chari R, Ter-Ovanesyan D, Haque SJ, Cecchi RJ, Kowal EJK, Buchthal J, et al. (2016). Comparison of Cas9 activators in multiple species. Nat. Methods 13, 563–567. [PubMed: 27214048]

Chen S, Lee AY, Bowens NM, Huber R, and Kravitz EA (2002). Fighting fruit flies: a model system for the study of aggression. Proc. Natl. Acad. Sci. USA 99, 5664–5668. [PubMed: 11960020]

Chiang AS, Lin CY, Chuang CC, Chang HM, Hsieh CH, Yeh CW, Shih CT, Wu JJ, Wang GT, Chen YC, et al. (2011). Three-dimensional reconstruction of brain-wide wiring networks in *Drosophila* at single-cell resolution. Curr. Biol 21, 1–11. [PubMed: 21129968]

Chiara V, Ramon Portugal F, and Jeanson R (2019). Social intolerance is a consequence, not a cause, of dispersal in spiders. PLoS Biol. 17, e3000319. [PubMed: 31265448]

Costa M, Manton JD, Ostrovsky AD, Prohaska S, and Jefferis GS (2016). NBLAST: rapid, sensitive comparison of neuronal structure and construction of neuron family databases. Neuron 91, 293–311. [PubMed: 27373836]

Craig W (1917). Appetites and aversions as constituents of instincts. Bio. Bulletin 34, 91–107.

Dana H, Sun Y, Mohar B, Hulse BK, Kerlin AM, Hasseman JP, Tsegaye G, Tsang A, Wong A, Patel R, et al. (2019). High-performance calcium sensors for imaging activity in neuronal populations and microcompartments. Nat. Methods 16, 649–657. [PubMed: 31209382]

Datta SR, Vasconcelos ML, Ruta V, Luo S, Wong A, Demir E, Flores J, Balonze K, Dickson BJ, and Axel R (2008). The *Drosophila* pheromone cVA activates a sexually dimorphic neural circuit. Nature 452, 473–477. [PubMed: 18305480]

Deutsch D, Pacheco DA, Encarnacion-rivera L, Pereira T, Fathy R, Ireland EC, Burke AT, Dorkenwald S, McKellar C, Macrina T, et al. (2020). The neural basis for a persistent internal state in Drosophila females. bioRxiv. DOI: 10.1101/2020.02.13.947952.

Duistermars BJ, Pfeiffer BD, Hoopfer ED, Anderson DJ, Duistermars BJ, Pfeiffer BD, Hoopfer ED, and Anderson DJ (2018). A brain module for scalable control of complex multi-motor threat displays. Neuron 100, 1474–1490. [PubMed: 30415997]

Dulac C, and Kimchi T (2007). Neural mechanisms underlying sex-specific behaviors in vertebrates. Curr. Opin. Neurobiol 17, 675–683. [PubMed: 18343651]

Eyjolfsdottir E, Branson S, Burgos-Artizzu XP, Hoopfer ED, Schor J, Anderson DJ, and Perona P (2014). Detecting social actions of fruit flies. Lect. Notes Comput. Sci 8690, 772–787.

Falkner AL, Dollar P, Perona P, Anderson DJ, and Lin D (2014). Decoding ventromedial hypothalamic neural activity during male mouse aggression. J. Neurosci 34, 5971–5984. [PubMed: 24760856]

Falkner AL, Grosenick LD, Thomas J, Deisseroth K, and Lin D (2016). Hypothalamic control of male aggression-seeking behavior. Nat. Neurosci 19, 596–604. [PubMed: 26950005]

Fernández MP, Chan YB, Yew JY, Billeter JC, Dreisewerd K, Levine JD, and Kravitz EA (2010). Pheromonal and behavioral cues trigger male-to-female aggression in *Drosophila*. PLoS Bio. 8, e1000541. [PubMed: 21124886]

Gao XJ, Riabinina O, Li J, Potter CJ, Clandinin TR, and Luo L (2015). A transcriptional reporter of intracellular Ca^{2+} in *Drosophila*. Nat. Methods 18, 917–925.

Gentry RN, Schuweiler DR, and Roesch MR (2019). Dopamine signals related to appetitive and aversive events in paradigms that manipulate reward and avoidability. Brain Res. 15, 80–90.

Hashikawa K, Hashikawa Y, Falkner A, and Lin D (2016). The neural circuits of mating and fighting in male mice. Curr. Opin. Neurobiol 38, 27–37. [PubMed: 26849838]

Hashikawa K, Hashikawa Y, Tremblay R, Zhang J, Feng JE, Sabol A, Piper WT, Lee H, Rudy B, and Lin D (2017). Esr1+cells in the ventromedial hypothalamus control female aggression. Nat. Neurosci 20, 1580–1590. [PubMed: 28920934]

Hobert O, and Kratsios P (2019). Neuronal identity control by terminal selectors in worms, flies, and chordates. Curr. Opin. Neurobiol 56, 97–105. [PubMed: 30665084]

Hong EJ, and Wilson RI (2015). Simultaneous encoding of odors by channels with diverse sensitivity to inhibition. Neuron 85, 573–589. [PubMed: 25619655]

Hoopfer ED (2016). Neural control of aggression in *Drosophila*. Curr. Opin. Neurobiol 38, 109–118. [PubMed: 27179788]

Hoopfer ED, Jung Y, Inagaki HK, Rubin GM, and Anderson DJ (2015). P1 interneurons promote a persistent internal state that enhances inter-male aggression in *Drosophila*. Elife 4, e11346. [PubMed: 26714106]

Hoyer SC, Eckart A, Herrel A, Zars T, Fischer SA, Hardie SL, and Heisenberg M (2008). Octopamine in male aggression of *Drosophila*. Curr. Biol 18, 159–167. [PubMed: 18249112]

Inagaki HK, Jung Y, Hoopfer ED, Wong AM, Mishra N, Lin JY, Tsien RY, and Anderson DJ (2014). Optogenetic control of freely behaving adult *Drosophila* using a red-shifted channelrhodopsin. Nat. Methods 11, 325–332. [PubMed: 24363022]

Ishii K, Wohl M, Desouza A, Asahina K, Diego S, and States U (2020). Sex-determining genes distinctly regulate courtship capability and target preference via sexually dimorphic neurons, Elife 9, e52701. [PubMed: 32314964]

Jenett A, Rubin GM, Ngo T-TB, Shepherd D, Murphy C, Dionne H, Pfeiffer BD, Cavallaro A, Hall D, Jeter J, et al. (2012). A GAL4-driver line resource for *Drosophila* neurobiology. Cell Rep. 2, 991–1001. [PubMed: 23063364]

Jennings JH, Ung RL, Resendez SL, Stamatakis AM, Taylor JG, Huang J, Veleta K, Kantak PA, Aita M, Shilling-Scrivo K, et al. (2015). Visualizing hypothalamic network dynamics for appetitive and consummatory behaviors. Cell 160, 516–527. [PubMed: 25635459]

Jung Y, Kennedy A, Chiu H, Mohammad F, Claridge-Chang A, and Anderson DJ (2020). Neurons that function within an integrator to promote a persistent behavioral state in *Drosophila*. Neuron 105, 1–12. [PubMed: 31951525]

Kabra M, Robie AA, Rivera-Alba M, Branson S, and Branson K (2013). JAABA: Interactive machine learning for automatic annotation of animal behavior. Nat. Methods 10, 64–67. [PubMed: 23202433]

Kim DW, Yao Z, Graybuck LT, Nguyen TN, Smith KA, Fong O, Yi L, Koulena N, Pierson N, Shah S, et al. (2019). Multimodal analysis of cell types in a hypothalamic node controlling social behavior. Cell 179, 713–728. [PubMed: 31626771]

Kimura K, Hachiya T, Koganezawa M, Tazawa T, and Yamamoto D (2008). Fruitless and doublesex coordinate to generate male-specific neurons that can initiate courtship. Neuron 59, 759–769. [PubMed: 18786359]

Klapoetke NC, Murata Y, Kim SS, Pulver SR, Birdsey-Benson A, Cho YK, Morimoto TK, Chuong AS, Carpenter EJ, Tian Z, et al. (2014). Independent optical excitation of distinct neural populations. Nat. Methods 11, 338–346. [PubMed: 24509633]

Koganezawa M, Kimura K.i., and Yamamoto D (2016). The neural circuitry that functions as a switch for courtship versus aggression in *Drosophila* males. Curr. Biol 26, 1395–1403. [PubMed: 27185554]

Kravitz EA, and Fernández MP (2015). Aggression in *Drosophila*. Beh. Neurosci 129, 549–563.

Lee H, Kim DW, Remedios R, Anthony TE, Chang A, Madisen L, Zeng H, and Anderson DJ (2014). Scalable control of mounting and attack by Esr1+ neurons in the ventromedial hypothalamus. Nature 509, 627–632. [PubMed: 24739975]

Lim RS, Eyjolfsdottir E, Shin E, Perona P, and Anderson DJ (2014). How food controls aggression in *Drosophila*. Plos One 9, e105626. [PubMed: 25162609]

Longair MH, Baker DA, and Armstrong JD (2011). Simple neurite tracer: Open source software for reconstruction, visualization and analysis of neuronal processes. Bioinformatics 27, 2453–2454. [PubMed: 21727141]

Lorenz K (1950). The comparative method in studying innate behavior patterns In Physiological Mechanisms in Animal Behavior. Society's Symposium IV (Oxford: Academic Press), 221–268.

Luo L, Callaway EM, and Svoboda K (2008). Genetic dissection of neural circuits. Neuron 57, 634–660. [PubMed: 18341986]

Manoli DS, Fan P, Fraser EJ, and Shah NM (2013). Neural control of sexually dimorphic behaviors. Curr. Opin. Neurobiol 23, 330–338. [PubMed: 23680385]

Masse NY, Cachero S, Ostrovsky AD, and Jefferis GS (2012). A mutual information approach to automate identification of neuronal clusters in *Drosophila* brain images. Front. Neuroinform 6, 21. [PubMed: 22675299]

McKellar CE, Lillvis JL, Bath DE, Fitzgerald JE, Cannon JG, Simpson JH, Dickson BJ, Mckellar CE, Lillvis JL, Bath DE, et al. (2019). Threshold-based ordering of sequential actions during *Drosophila* courtship. Curr. Biol 29, 426–434. [PubMed: 30661796]

Mohammad F, Stewart JC, Ott S, Chlebikova K, Chua JY, Koh TW, Ho J, and Claridge-Chang A (2017). Optogenetic inhibition of behavior with anion channelrhodopsins. Nat. Methods 14, 271–274. [PubMed: 28114289]

Nilsen SP, Chan Y-B, Huber R, and Kravitz EA (2004). Gender-selective patterns of aggressive behavior in *Drosophila melanogaster*. Proc. Natl. Acad. Sci. USA 101, 12342–12347. [PubMed: 15302936]

Palavicino-Maggio CB, Chan YB, McKellar C, and Kravitz EA (2019). A small number of cholinergic neurons mediate hyperaggression in female *Drosophila*. Proc. Natl. Acad. Sci. USA 116, 17029–17038. [PubMed: 31391301]

Pavlou HJ, Lin AC, Neville MC, Nojima T, Diao F, Chen BE, White BH, and Goodwin SF (2016). Neural circuitry coordinating male copulation. ELife 5, e20713. [PubMed: 27855059]

Pfeiffer BD, Jenett A, Hammonds AS, Ngo TTB, Misra S, Murphy C, Scully A, Carlson JW, Wan KH, Laverty TR, et al. (2008). Tools for neuroanatomy and neurogenetics in *Drosophila*. Proc. Natl. Acad. Sci. USA 105, 9715–9720. [PubMed: 18621688]

Pfeiffer BD, Ngo T-TB, Hibbard KL, Murphy C, Jenett A, Truman JW, and Rubin GM (2010). Refinement of tools for targeted gene expression in *Drosophila*. Genetics 186, 735–755. [PubMed: 20697123]

Remedios R, Kennedy A, Zelikowsky M, Grewe BF, Schnitzer MJ, and Anderson DJ (2017). Social behaviour shapes hypothalamic neural ensemble representations of conspecific sex. Nature 550, 388–392. [PubMed: 29052632]

Rezával C, Nojima T, Neville MC, Lin AC, and Goodwin SF (2014). Sexually dimorphic octopaminergic neurons modulate female postmating behaviors in *Drosophila*. Curr. Biol 24, 725–730. [PubMed: 24631243]

Rideout EJ, Dornan AJ, Neville MC, Eadie S, and Goodwin SF (2010). Control of sexual differentiation and behavior by the *doublesex* gene in *Drosophila melanogaster*. Nat. Neurosci 13, 458–467. [PubMed: 20305646]

Ruta V, Datta SR, Vasconcelos ML, Freeland J, Looger LL, and Axel R (2010). A dimorphic pheromone circuit in *Drosophila* from sensory input to descending output. Nature 468, 686–690. [PubMed: 21124455]

Salamone JD, and Correa M (2012). The mysterious motivational functions of mesolimbic dopamine. Neuron 76, 470–485. [PubMed: 23141060]

Schretter CE, Aso Y, Robie AA, Dreher M, Dolan M-J, Chen N, Ito M, Yang T, Parekh R, Branson KM, et al. (2020). Cell types and neuronal circuitry underlying female aggression in *Drosophila*. eLife, e58942. [PubMed: 33141021]

Shelly TE (1999). Defense of oviposition sites by female oriental fruit flies (Diptera: Tephritidae). Florida Entomol. 82, 339–346.

Sgoifo A, Stilli D, Musso E, Mainardi D, and Parmigiani S (1992). Offensive and defensive bite-target topographies in attacks by lactating rats. Aggress. Behav 21, 79–89.

Stockinger P, Kvitsiani D, Rotkopf S, Tirián L, and Dickson BJ (2005). *Drosophila* Male Courtship Behavior. Cell 121, 795–807. [PubMed: 15935765]

Tinbergen N (1951). The study of instinct (Clarendon Press/Oxford University Press).

Toth M, Halasz J, Mikics E, Barsy B, and Haller J (2008). Early social deprivation induces disturbed social communication and violent aggression in adulthood. Behav. Neurosci 122, 849–854. [PubMed: 18729638]

Ueda A, and Kidokoro Y (2002). Aggressive behaviours of female *Drosophila melanogaster* are influenced by their social experience and food resources. Physiol. Entomol 27, 21–28.

von Philipsborn AC, Liu T, Yu JY, Masser C, Bidaye SS, and Dickson BJ (2011). Neuronal control of *Drosophila* courtship song. Neuron 69, 509–522. [PubMed: 21315261]

Vrontou E, Nilsen SP, Demir E, Kravitz EA, and Dickson BJ (2006). *fruitless* regulates aggression and dominance in *Drosophila*. Nat. Neurosci 9, 1469–1471. [PubMed: 17115036]

Wang F, Wang K, Forknall N, Patrick C, Yang T, Parekh R, Bock D, and Dickson BJ (2020). Neural circuitry linking mating and egg laying in *Drosophila* females. Nature 579, 101–105. [PubMed: 32103180]

Wang L, Dankert H, Perona P, and Anderson DJ (2008). A common genetic target for environmental and heritable influences on aggressiveness in *Drosophila*. Proc. Natl. Acad. Sci. USA 105, 5657–5663. [PubMed: 18408154]

Watanabe K, Chiu H, Pfeiffer BD, Wong AM, Hoopfer ED, Rubin GM, and Anderson DJ (2017). A circuit node that integrates convergent input from neuromodulatory and social behavior-promoting neurons to control aggression in *Drosophila*. Neuron 95, 1112–1128. [PubMed: 28858617]

Yamamoto D, and Koganezawa M (2013). Genes and circuits of courtship behaviour in *Drosophila* males. Nat. Rev. Neurosci 14, 681–692. [PubMed: 24052176]

Yang CF, Chiang MC, Gray DC, Prabhakaran M, Alvarado M, Juntti SA, Unger EK, Wells JA, and Shah NM (2013). Sexually dimorphic neurons in the ventromedial hypothalamus govern mating in both sexes and aggression in males. Cell 153, 896–909. [PubMed: 23663785]

Yang CF, and Shah NM (2014). Representing sex in the brain, one module at a time. Neuron 82, 261–278. [PubMed: 24742456]

Yu JY, Kanai MI, Demir E, Jefferis GS, and Dickson BJ (2010). Cellular organization of the neural circuit that drives *Drosophila* courtship behavior. Curr. Biol 20, 1602–1614. [PubMed: 20832315]

Zelikowsky M, Hui M, Karigo T, Choe A, Yang B, Blanco MR, Beadle K, Gradinaru V, Deverman BE, and Anderson DJ (2018). The neuropeptide Tac2 controls a distributed brain state induced by chronic social isolation stress. Cell 173, 1265–1279. [PubMed: 29775595]

RESEARCH HIGHLIGHTS

- Sexually dimorphic attack is controlled by sexually dimorphic neurons in *Drosophila*
- Shared cells that control aggressive approach activate the dimorphic attack neurons
- The transition from approach to attack occurs at a higher threshold than approach
- Isolation enhances shared→dimorphic functional connectivity to promote aggression

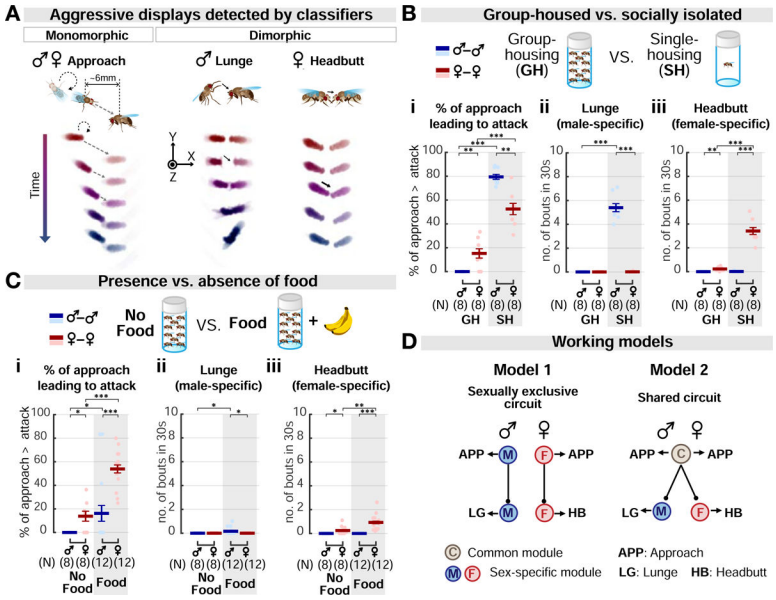

Figure 1. Contextual influences on sexually monomorphic and dimorphic aggressive actions in males and females

(A) Example bouts detected by automated behavioral classifiers. Approach: fly orients and moves towards target. Lunge: fly raises its upper body and slams down onto target. Headbutt: fly thrusts its body towards the target and strikes it with its head. See also Figure S1.

(B-C) Effects of social isolation (B) and food presence (C) on male vs. female aggression. (B) Testers were reared either in groups (GH; 20 flies/vial) or in isolation (SH; 1 fly/vial) for 6 days prior to test. In (C), a banana chunk (“Food”) was provided during testing of GH flies. Dark lines: mean±SEM. Light circles: individual data. Here and throughout, ns, not significant; *p<0.05; **p<0.01; and ***p<0.001. Full genotypes of experimental flies for this and subsequent figures are listed in Table S1. Statistical data are listed in Table S3.

(D) Proposed models for aggression circuitry in males and females. Model 1, the aggression circuit in each sex is composed exclusively of sex-specific components. Model 2, some aggression circuit components, controlling similar behaviors, are shared by both sexes.

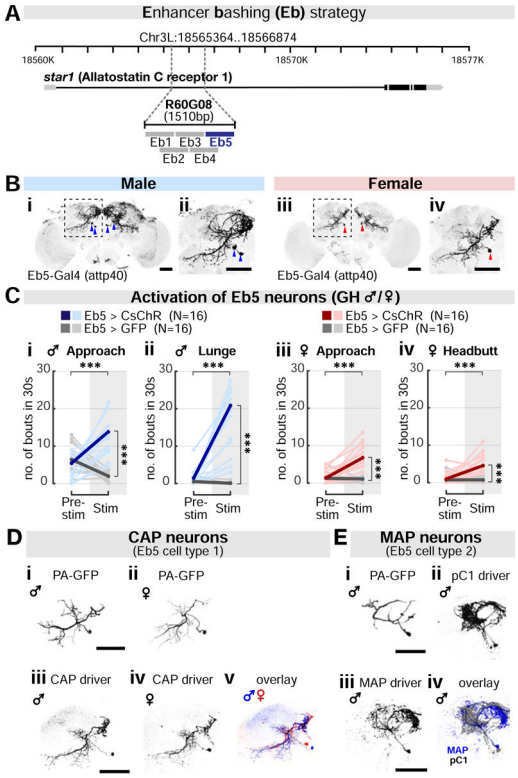

Figure 2. Identification of sexually monomorphic and dimorphic aggression-promoting cell types

(A) "Enhancer-bashing" strategy to identify GAL4 drivers for R60G08 subpopulations.

(B) Neurons labeled by Eb5-Gal4 (attp40) in males (i-ii) and females (iii-iv). Areas outlined by dashed boxes in (i) and (iii) are enlarged in (ii) and (iv), respectively. Arrowheads: cell body locations. Scale bar: 50μm. See also Figures S3A and S4B.

(C) Activation of Eb5 neurons strongly promotes male (i-ii) and female aggression (iii-iv). Shown are bouts of approach (i and iii), lunging (ii) and headbutting (iv). Light and dark color lines: individual data and the mean, respectively. See also Figure S3B.

(D) Morphology of the sexually shared CAP neurons in males and females. Neuronal traces labelled by activated photo-activatable (PA) GFP (i-ii), CsChrimson expression driven by CAP driver (iii-iv; Eb5-Gal4 (attp40); R22F05-Gal80(attp2)), and overlay between sexes (v). Scale bar: 50μm. See also Figure S3C–E.

(E) Morphology of the male-specific MAP neurons in males. Neuronal traces labelled by activated PA-GFP (i), CsChrimson expression driven by pC1 driver (ii; NP2631/dsx-Flp), or by MAP driver (iii; Eb5-AD(vk27), R22F05-DBD(attp2)) and overlay between pC1 and MAP (iv). Scale bar: 50μm. See also Figure S4A–D.

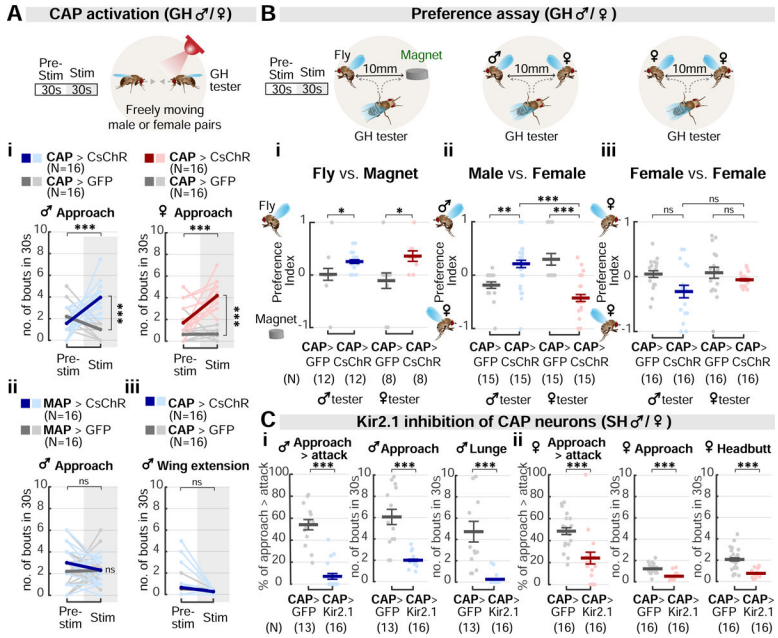

Figure 3. CAP stimulation evokes aggressive approach in males and females

(A) CAP activation in GH males and females (i), but not MAP activation in males (ii), promotes approach. Courtship, measured by bouts of wing extension, is not affected by CAP stimulation (iii). Light and dark color lines: individual data and the mean, respectively.

(B) Analysis of approach preference in CAP-stimulated testers towards: (i) flies vs. an inanimate object (magnet); (ii) same- vs. opposite-sex fly targets; and (iii) two female fly targets. The preference index (PI): (i) PI = ($n_{\text{toward the fly target}} - n_{\text{toward the magnet}}$) / n_{total}; (ii), PI = ($n_{\text{toward the male target}} - n_{\text{toward the female target}}$) / n_{total}; (iii), PI = ($n_{\text{toward the left female target}} - n_{\text{toward the right female target}}$) / n_{total}. See also Methods. Dark lines: mean±SEM. Light circles: individual data.

(C) Silencing of CAP neurons using Kir2.1 reduces naturally-occurring aggression in SH males (i) and females (ii). Dark lines: mean±SEM. Light circles: individual data.

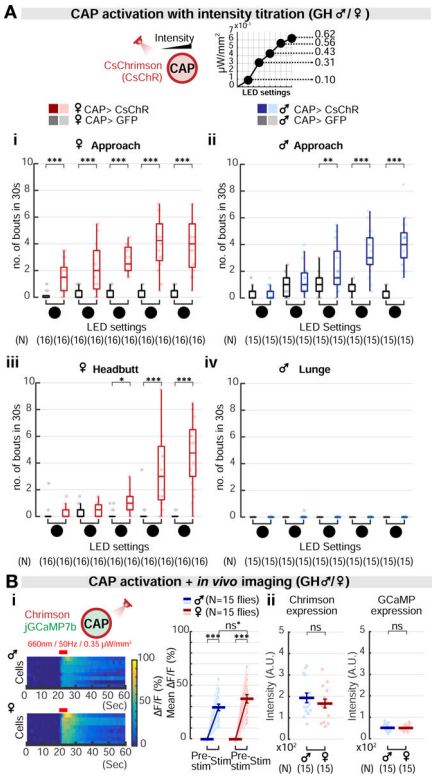

Figure 4. Aggression-promoting thresholds for CAP activation differ in males and females

(A) Optogenetic activation of CAP neurons at five increasing intensities of photostimulation in females (i, iii) and males (ii, iv), with dependent variables of approach (i, ii) headbutt (iii) or lunge (iv). The intensities of the stimulation (❶-❺) correspond to 0.1, 0.31, 0.43, 0.56, 0.62 μW/mm^2. Light circles: individual data.

(B) (i) GCaMP fluorescence changes (ΔF/F) in CAP neurons in response to photo-simulation of the same cells, in males versus females. Red bar: 5 seconds of 660nm photostimulation. Light circles: individual data. Dark lines: mean±SEM. ns*: non-significant after the Bonferroni correction. (ii) Expression level of Chrimson::tdTomato or GCaMP7b in male and female CAP neurons, measured by fluorescence intensity.

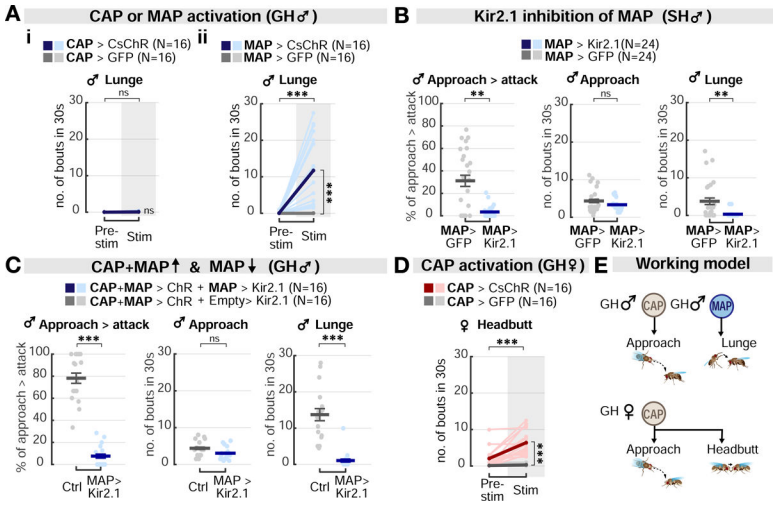

Figure 5. MAP and CAP stimulation elicits dimorphic attacks in males and females, respectively

(A) Optogenetic stimulation of MAP neurons alone, but not of CAP neurons, is sufficient to evoke lunging in GH males. Light and dark colored lines: individual data and the mean, respectively.

(B) Kir2.1 inhibition of MAP neurons in SH males reduces spontaneous lunges but does not affect approaches towards a male target. Dark lines: mean±SEM. Light circles: individual data.

(C) MAP silencing suppresses lunging promoted by co-activation of CAP and MAP cells, but does not reduce approach, in GH males. Dark lines: mean±SEM. Light circles: individual data.

(D) CAP stimulation is sufficient to evoke headbutting in GH females. Light and dark color lines: individual data and the mean, respectively.

(E) Summary of the behavioral phenotypes produced by CAP or MAP stimulation in GH flies. In males (upper), CAP stimulation promotes approach, whereas MAP stimulation triggers lunging. In females (lower), CAP stimulation promotes approach and headbutting.

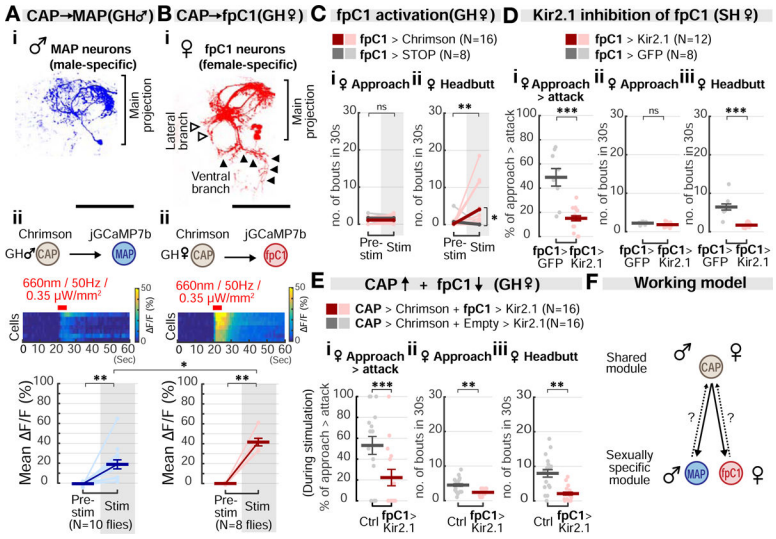

Figure 6. Functional connectivity between monomorphic and dimorphic circuit modules

(A) Morphology of MAP neurons (i) and jGCaMP7b fluorescence changes (ii) in response to CAP stimulation in GH male flies. Light circles: individual data. Dark lines: mean±SEM. Fig. 6Ai is duplicated from Fig. 2Eiii for purposes of comparison between MAP and fpC1 neurons. Scale bar: 50μm. Mann-Whitney U test, corrected for multiple comparisons.

(B) Morphology of fpC1 neurons (i) and jGCaMP7b fluorescence changes (ii) in response to CAP stimulation in GH females. Light circles: individual data. Dark lines: mean±SEM. Scale bar: 50μm. Mann-Whitney U test, corrected for multiple comparisons.

(C) Optogenetic activation of fpC1 neurons promotes headbutting, but not approach, in GH females. Light and dark color lines: individual data and the means, respectively. See also Figures S4E and S5D.

(D) Inactivation of fpC1 neurons with Kir2.1 expression. Dark lines: mean±SEM. Light circles: individual data.

(E) Behavioral epistasis between the upstream CAP neurons and the downstream fpC1 neurons. Dark lines: mean±SEM. Light circles: individual data.

(F) Summary of circuit connectivity in males and females. Sexually monomorphic CAP neurons functionally connect with dimorphic MAP and fpC1 neurons in males and females, respectively. Dashed arrow: potential feedback from MAP/fpC1 onto CAP.

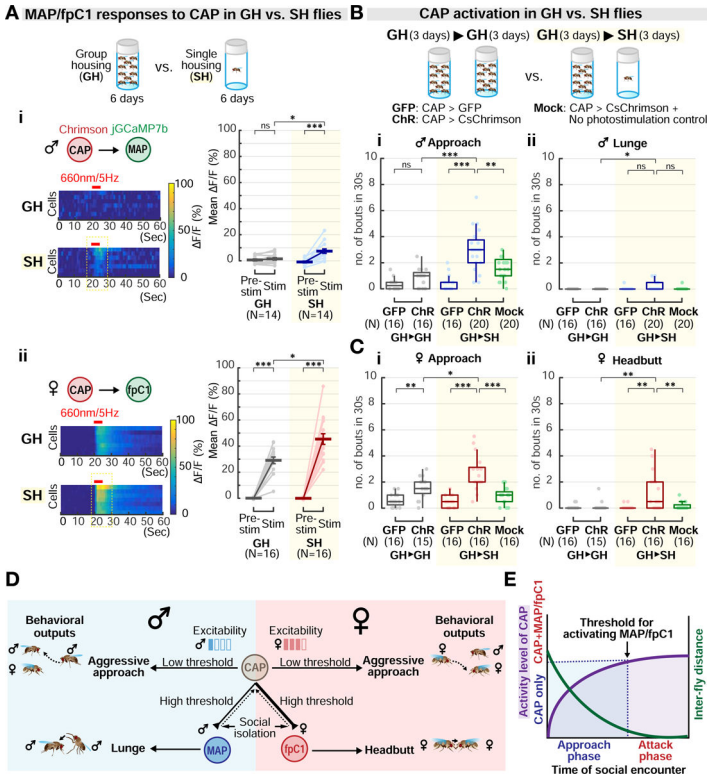

Figure 7. Social isolation enhances aggressiveness by strengthening circuit functional connectivity

(A) jGCaMP7b fluorescence changes in MAP (i) or fpC1 neurons (ii) in response to CAP stimulation in group-housed (GH) or single-housed (SH) flies. Mann-Whitney U test, corrected for multiple comparisons. Light circles: individual data. Dark lines: mean±SEM.

(B-C) Optogenetic activation of CAP neurons in flies reared in groups for 6 days (GH>GH) or in groups for 3 days followed by isolation for 3 days (GH>SH). “GFP,” CAP>GFP control; “ChR,” CAP>CsChrimson with photostimulation; “Mock,” CAP>CsChrimson without photostimulation. Light circles: individual data.

(D) Diagram illustrating circuit control of sexually monomorphic and dimorphic phases of aggression. Sexually shared CAP neurons control appetitive (approach) and trigger consummatory (lunge vs. headbutt) aggressive behavior via MAP or fpC1 neurons in males vs. females, respectively. Low vs. High threshold: the relative light intensities used for CAP stimulation to elicit appetitive vs. consummatory behavior, respectively. MAP or fpC1 stimulation promotes attack independently of approach. The CAP→MAP/fpC1 connectivity is a locus for experience-dependent enhancement of aggression. The synaptic connectivity underlying the functional connection between CAP and MAP/fpC1 may be direct or indirect. Dashed arrows: potential feedback from MAP/fpC1 onto CAP.

(E) Model showing how progression from the approach to attack phases of aggression might be controlled by a ramp-up in CAP activity, from below to above threshold for MAP/fpC1 activation (arrow). CAP activity is predicted to vary inversely with distance between flies, for example due to an increase in the intensity of sensory cues.

KEY RESOURCES TABLE

REAGENT or RESOURCE	SOURCE	IDENTIFIER
Antibodies		
anti-GFP(rabbit)	Thermo Fisher Scientific	Cat#A11122; RRID: AB_221569
anti-RFP(rat)	ChromoTek	Cat#5f8–100; RRID:AB_2336064
nc82(mouse)	Developmental Studies Hybridoma Bank	Cat#nc82; RRID:AB_2314866
anti-Cadherin(extracellular domain; rat)	Developmental Studies Hybridoma Bank	Cat#DN-Ex #8; RRID:AB_528121
anti-FruM(rabbit)	Barry J. Dickson Lab; Stockinger et al., 2005	N/A
Goat anti-rabbit IgG(H+L) Alexa Fluor 488	Thermo Fisher Scientific	Cat#A11008; RRID: AB_143165
Goat anti-rat IgG(H+L) Alexa Fluor 568	Thermo Fisher Scientific	Cat#A11077; RRID: AB_2534121
Goat anti-mouse IgG(H+L) Alexa Fluor 633	Thermo Fisher Scientific	Cat#A21050; RRID: AB_141431
Goat anti-rat IgG(H+L) Alexa Fluor 647	Thermo Fisher Scientific	Cat#A21247; RRID: AB_141778
Normal Goat Serum	Jackson ImmunoResearch INC.	Cat#005-000-121; RRID: AB_2336990
Chemicals, Peptides, and Recombinant Proteins		
VECTASHIELD Antifade Mounting Media	VECTOR Laboratories	Cat#H-1000; RRID: AB_2336789
Paraformaldehyde, 16% solution, EM grade	Electron Microscopy Sciences	Cat#15710; CAS no. 30525-89-4
All trans-Retinal (powder, ≥98%)	Sigma-Aldrich	Cat#R2500; CAS no.116-31-4
Insect-A-Slip	BioQuip Products	Cat#2871B
Hydrocarbon Soluble Siliconizing Fluid	ThermoFisher Scientific	Cat#TS-42800; CAS no.474-02-4
Experimental Models: Organisms/Strains		
Drosophila: Wild-type Canton S	Heisenberg lab ; Hoyer et al., 2008	N/A
Drosophila: *R60G08-Gal4 (attp2)*	Rubin Lab	RRID:BDSC_39260
Drosophila: *pBDPGAL4U (attp2)*	Rubin Lab	RRID:BDSC_68384
Drosophila: *Eb2-Gal4 (attp2)*	This study	N/A
Drosophila: *Eb3-Gal4 (attp2)*	This study	N/A
Drosophila: *Eb4-Gal4 (attp2)*	This study	N/A
Drosophila: *Eb5-Gal4 (attp2)*	This study	N/A
Drosophila: *Eb5-Gal4 (attp40)*	This study	N/A
Drosophila: BDP-p65AD(attp40)	Rubin Lab	N/A
Drosophila: BDP-Gal4DBD(attp2)	Rubin Lab	N/A
Drosophila: *Eb5-Gal80 (attp2)*	This study	N/A
Drosophila: *Eb5-p65AD (vk27)*	This study	N/A
Drosophila: Eb5-iLexA(attp18)	This study	N/A
Drosophila: R22F05-Gal4DBD(attp2)	Rubin Lab	RRID:BDSC_69772
Drosophila: *R22F05-LexADBD (attp2)*	This study	N/A
Drosophila: *R22F05-Gal80 (attp2)*	This study	N/A

REAGENT or RESOURCE	SOURCE	IDENTIFIER
Drosophila: *R26E01-Gal4 (attp2)*	Bloominton Drosophila Stock Center	RRID:BDSC_60510
Drosophila: *R26E01-p65AD (attp40)*	Bloominton Drosophila Stock Center	RRID:BDSC_75740
Drosophila: dsx-Gal4	Goodwin Lab; Rideout et al., 2010	N/A
Drosophila: *dsx*-DBD	Goodwin Lab; Pavlou et al., 2016	N/A
Drosophila: dsx-Flp	Goodwin Lab; Rezával et al., 2014	N/A
Drosophila: *NP2631; dsx-Flp*	Koganezawa et al., 2016	N/A
Drosophila: otd-nls::FLPo(attp40)	Anderson Lab; Watanabe et al., 2017	N/A
Drosophila: Tk-Gal4[1]	Anderson Lab; Asahina et al., 2014	RRID:BDSC_51975
Drosophila: *20xUAS-IVS-CsChrimson.mVenus (attp2)*	Jayaraman Lab; Klapoetke et al., 2014	RRID:BDSC_55136
Drosophila: pJFRC82-*20xUAS-IVS-Syn21-GFP-p10 (attp2)*	Rubin Lab	N/A
Drosophila: pJFRC49-*10xUAS-eGFP::Kir2.1 (attp2)*	Rubin Lab	N/A
Drosophila: pJFRC81-*10xUAS-IVS-Syn21-GFP-p10 (attp2)*	Rubin Lab	N/A
Drosophila: 20xUAS-FRT-myrTopHat2-FRT-Chrimson-tdTomato-3.1(vk5)	Rubin Lab; Duistermars et al., 2018	N/A
Drosophila: 20xUAS-FRT-Chrimson-tdTomato-3.1-FRT-myrTopHat2 (vk5)	This study	N/A
Drosophila: *20xUAS-IVS-Syn21-Chrimson-tdTomato-3.1 (su(Hw)attp5)*	Gerald M. Rubin Lab; Watanabe et al., 2017	N/A
Drosophila: *20xUAS-IVS-Syn21-Chrimson-tdTomato-3.1 (vk5)*	Gerald M. Rubin Lab	N/A
Drosophila: *UAS-C3PA-GFP (III)*	Datta et al., 2008; Ruta et al., 2010	N/A
Drosophila: *20xUAS-IVS-jGCaMP7b(vk5)*	Bloominton Drosophila Stock Center; Dana et al., 2019	RRID:BDSC_79029
Drosophila: *13xLexAop-IVS-jGCaMP7b(vk5)*	Bloominton Drosophila Stock Center; Dana et al., 2019	RRID:BDSC_80915
Drosophila: 13xLexAop2-IVS-Syn21-CsChrimson-tdTomato-3.1(vk5)	Rubin Lab	N/A
Drosophila: 13xLexAop2-IVS-Syn21-Chrimson-tdTomato-3.1(su(Hw)attp5)	Rubin Lab	N/A
Drosophila: 13xLexAop2-eGFP::Kir2.1(attp40)	Rubin Lab	N/A
Drosophila: 10xUAS-nls::tdTomato(vk22)	Rubin Lab; Jung et al., 2020	N/A
Drosophila: 13xLexAop2-nls::GFP(vk40)	Rubin Lab; Jung et al., 2020	N/A
Oligonucleotides		
Eb1_F: caccatccttcccacttgagctccacagc	This study	N/A
Eb1_R: agttccattcactgtgggcaatgaaacgtc	This study	N/A
Eb2_F: caccggtgcaagatagtcaatcgttgcac	This study	N/A
Eb2_R: ctgagccaaaacacatgtgggggttattg	This study	N/A
Eb3_F: caccgacgtttcattgcccacagtgaatggaact	This study	N/A
Eb3_R: aaattgctcacagcttgacacgtccaac	This study	N/A

REAGENT or RESOURCE	SOURCE	IDENTIFIER
Eb4_F: cacccaataacccccacatgtgttttggctcag	This study	N/A
Eb4_R: ttactgactttctgagaaatcccctcg	This study	N/A
Eb5_F: caccgttggacgtgtcaagctgtgagcaattt	This study	N/A
Eb5_R: caattggtgataagtattcaaatggaattaagttaagtctacaag	This study	N/A
Recombinant DNA		
pBPGUw	Pfeiffer et al., 2008	RRID:Addgene_17575
pBPp65ADZpUw	Pfeiffer et al., 2010	RRID:Addgene_26234
pBPZpGal4DBDUw	Pfeiffer et al., 2010	RRID:Addgene_26233
pBPGAL80Uw-6	Pfeiffer et al., 2010	RRID:Addgene_26236
pattB-nsyb-MKII::nlsLexADBDo	Gao et al., 2015	RRID:Addgene_64725
pBPnlsLexA::p65Uw	Pfeiffer et al., 2010	RRID:Addgene_26230
pBPnlsLexA::p65::GADUw	This study	N/A
Software and Algorithms		
JFRCtemplate2010	Jenett et al., 2012	https://github.com/VirtualFlyBrain/DrosAdultBRAINdomains
Caltech FlyTracker	Eyjolfsdottir et al., 2014	http://www.vision.caltech.edu/Tools/FlyTracker/
Janelia Automatic Animal Behavior Annotator (JAABA)	Kabra et al., 2013	http://jaaba.sourceforge.net/
MATLAB R2014a and R2016a	MathWorks	RRID: SCR_001622
Fiji	https://fiji.sc/	RRID: SCR_002285
ApE-A plasmid Editor	M. Wayne Davis	https://jorgensen.biology.utah.edu/wayned/ape/
Computational Morphometry Toolkit (CMTK)	Masse et al., 2012	https://www.nitrc.org/projects/cmtk
Simple Neurite Tracer	Longair, M.H. et al., 2011	https://imagej.net/Simple_Neurite_Tracer
NBLAST	Costa et al., 2016	http://nblast.virtualflybrain.org:8080/NBLAST_on-the-fly/
FlyCircuit 1.2	Chiang et al., 2011	http://www.flycircuit.tw/
Adobe Photoshop CC 2015	Adobe Inc.	RRID:SCR_014199